Figure 2. Pollen tubes.
An *Arabidopsis* pistil with pollen tubes growing down towards the ovules. The pistil is stained with decolorized aniline blue to visualize the pollen tubes. (Photo: Dr. Yuan Chen.)

makes sense that wind-pollinated plants would make a lot of pollen, to increase the chance of finding a female, but even in self-pollinated plants, such as tomato, each anther makes many more pollen grains than are needed for the available females in that flower. Pollen competition (i.e. faster growing pollen tubes succeed) might explain this conundrum.

How do I find out more?

Carlson, A.L., Fitz Gerald, J.N., Telligman, M., Roshanmanesh, J., and Swanson, R.J. (2011). Defining the genetic architecture underlying female- and male-mediated nonrandom mating and seed yield traits in Arabidopsis. Plant Physiol. *157*, 1956–1964.

Cheung, A.Y., and Wu, H.-M. (2008). Structural and signaling networks for the polar cell growth machinery in pollen tubes. Annu. Rev. Plant Biol. *59*, 547–572.

Dobritsa, A.A., and Coerper, D. (2012). The novel plant protein INAPERTURATE POLLEN1 marks distinct cellular domains and controls formation of apertures in the *Arabidopsis* pollen exine. Plant Cell *24*, 4452–4464.

Okuda , S. Tsutsui, H., Shiina, K., Sprunck, S., Takeuchi, H., Yui, R., Kasahara, R.D., Hamamura, Y., Mizukami, A., Susaki, D. *et al.* (2009). Defensin-like polypeptide LUREs are pollen tube attractants secreted from synergid cells. Nature *458*, 357–361.

Petrovska, N., Wu, X., Donato, R., Wang, Z., Ong, E.-K., Jones, E., Forster, J., Emmerling, M., Sidoli, A., O'Hehir, R. and Spangenberg, G. (2004). Transgenic ryegrasses (Lolium spp.) with down-regulation of main pollen allergens. Mol. Breed. *14*, 489–501.

Qin, P. Ting, D., Shieh, A. and McCormick, S. (2012). Callose plug deposition patterns vary in pollen tubes of *Arabidopsis* thaliana ecotypes and tomato species. BMC Plant Biol. *12*, 178.

Tang, W., Ezcurra, I., Muschietti, J. and McCormick, S. (2002). A cysteine-rich extracellular protein, LAT52, interacts with the extracellular domain of the pollen receptor kinase LePRK2. Plant Cell *14*, 2277–2287.

Plant Gene Expression Center, USDA/ARS, University of California-Berkeley, 800 Buchanan St, Albany, CA, USA.
E-mail: sheilamc@berkeley.edu

Vision and the light environment

Eric J. Warrant[1,*] and Sönke Johnsen[2]

Almost all animals, no matter how humble, possess eyes. Only those that live in total darkness, such as in a pitch-dark cave, may lack eyes entirely. Even at tremendous depths in the ocean — where the only lights that are ever seen are rare and fitful sparks of bioluminescence — most animals have eyes, and often surprisingly well-developed eyes. And despite their diversity (there are currently ten generally recognised optical types) all eyes have evolved in response to the remarkably varied light environments that are present in the habitats where animals live. Variations in the intensity of light, as well as in its direction, colour and dominant planes of polarisation, have all had dramatic effects on visual evolution. In the terrestrial habitats where we ourselves have most recently evolved, the light environment can vary quite markedly from day to night and from one location to another. In aquatic habitats, this variation can be orders of magnitude greater. Even though the ecologies and life histories of animals have played a major role in visual evolution, it is arguably the physical limitations imposed on photodetection by a given habitat and its light environment that have defined the basic selective pressures that have driven the evolution of eyes.

Terrestrial light environments

The light experienced by day-active (diurnal) terrestrial animals is completely dominated by direct and indirect light from the sun, which behaves approximately as a celestial blackbody radiator. Like all blackbody radiators, the spectrum of light emitted by the sun characteristically depends on its surface temperature (around 5800 °K), although before reaching the Earth's surface this broad spectrum is narrowed by absorption in the ultraviolet (UV) and the infrared (by the filtering affects of the ozone layer, water vapour and other atmospheric constituents). As a result of atmospheric (Rayleigh) scattering of this sunlight — which is much greater at shorter wavelengths — the wide dome of the sky, whilst considerably dimmer (per unit area) than the sun, is also substantially bluer. Because of its much larger size compared to the disc of the sun, the blue sky contributes a significant fraction of the shorter wavelength light seen by diurnal animals (light in the 300–500 nm range) and affects the final measured spectrum of skylight irradiance (Figure 1A).

Scattered skylight is also linearly polarised, with the exact direction of each light ray's electric field vector, and its degree of polarisation, varying systematically across the dome of the sky. Rayleigh scattering thus creates a distinct pattern of skylight polarisation, within which the electric field vectors are approximately arranged in concentric circles around the sun. The pattern has a symmetry plane defined by the solar meridian, the semicircular line that traverses the entire dome of the sky (from horizon to horizon) and contains both the sky's zenith (the point directly above the observer) and the sun. This symmetry allows many terrestrial and shallow-living aquatic animals — particularly invertebrates — to use the polarisation pattern as a visual celestial compass during navigation.

As the sun's elevation declines from its highest at midday (60–90°) to 0° at sunset, the daylight intensity drops approximately 100-fold, most of this drop occurring in the final 5°. By the time the sun has further sunk to 18° below the horizon (signalling the end of astronomical twilight and the onset of true night), light levels on a moonless night will have fallen a further 1–10 million times, although a night lit by a full moon will be around 100–1000 times brighter than this minimum. As we ourselves can attest, vision during the day and even at brighter twilight levels is reliable and of high quality. But at night our visual abilities are severely impaired by the paucity of light. We lose our ability to see colour (a loss likely shared by practically all other vertebrates) and

the contrasts of fine spatial details are drowned by visual noise in our photoreceptors.

Remarkably though, many nocturnal animals see much better than we do at night, thanks to an impressive suite of optical and neural adaptations possessed by their visual systems. Certain nocturnal insects are able to distinguish colour, to orient using the faint pattern of polarised light formed in the moonlit sky and to navigate and home using landmarks or the broad but faint stripe of the Milky Way. Nocturnal vertebrates, like the Western tarsier *Cephalopachus bancanus*, with its massive eyes, are likely to share several of these abilities. However, whether colour vision is one of them is still an open question. Another nocturnal primate, the owl monkey *Aotus azarae*, has abandoned the trichromacy common in diurnal higher primates like ourselves: they have lost two spectral classes of cone photoreceptors to become monochromats, presumably to gain greater sensitivity.

The transitions from day to night and night to day (and from moonrise to moonset) are accompanied by the most dramatic changes in the colour of daylight experienced in terrestrial habitats (Figure 1A). As the sun or moon drops close to the horizon, skylight is typically dominated by longer wavelengths, that is, it has the orange-red colour we associate with sunsets. But as the sun or moon falls to just a few degrees below the horizon, the sky instead becomes intensely blue (Figure 1A). This is because the low elevation of the celestial body forces direct light to travel a long way through the atmosphere, causing longer wavelengths to be filtered out by the intervening ozone. As the sun or moon sets further, the blue twilight fades and, if both bodies are absent, is replaced by a dimmer and redder light: this light comes from the stars (particularly those we cannot see, which are dominated by red dwarfs emitting long wavelength light), and from airglow (which causes sharp peaks in the 'starlight' spectrum; Figure 1A).

The redder illumination of moonless nights is clearly seen in Figure 1B, which is an image of Death Valley in California obtained

at night with a 62 second exposure. The landscape is distinctly orange, although we ourselves, lacking colour vision at night, would fail to notice this. A landscape bathed in moonlight, in contrast, looks remarkably similar to the same landscape bathed in sunlight (Figure 1C). This is because moonlight is simply reflected sunlight, with the moon behaving as a dirty and somewhat brown mirror that redirects the sun's rays while slightly red-shifting their spectrum.

How nocturnal animals deal with these colour shifts in nocturnal light is not known, but these changes are likely within those tolerated by colour constancy, the neural mechanisms that ensure that the perception of colour remains uncorrupted during changes in the spectrum of natural illumination. What is unclear, however, is whether nocturnal animals are equally tolerant of light pollution. Apart from drastically increasing nocturnal irradiance, most light pollution is generated by mercury bulbs and low- and high-pressure sodium lamps whose spectra are significantly red-shifted, thus creating our orange and starless nights. Little is known of how light pollution impacts visual behaviour in nocturnal animals, although some well-known cases nonetheless exist. Sea-turtle hatchlings, programmed to seek out and scramble towards the faint glimmer of light marking the sea, are often misguided by the lights of nearby beach resorts, frequently perishing in their frantic and futile attempts to reach the water.

Although less dramatic, quite large changes in the spectrum of daylight can also occur within forests. On a sunny day in light woodland, where extensive clearings are formed by wide gaps in the forest canopy, the spectrum of irradiance in the clearings is similar to that in an open field. As the gaps close, direct light from the sun becomes blocked, and shade increases. The spectrum of irradiance then becomes shifted to shorter wavelengths since light penetrating the canopy gaps tends to originate predominantly from the blue sky. Once the gaps close completely, the irradiance spectrum at the forest floor is dominated by the
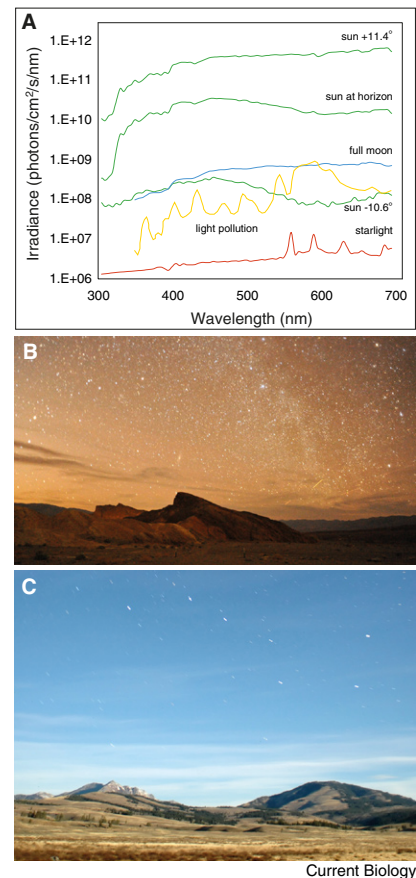
Current Biology

Figure 1. The spectral properties of light in terrestrial habitats.
(A) The irradiance spectra of sunlight (*green curves*), moonlight (*blue curve*), starlight (*red curve*) and light pollution (*yellow curve*) in a terrestrial habitat (spectra were measured on a near-cloudless night). Sunlight spectra are shown just prior to sunset (sun elevation +11.4°), at sunset (sun at horizon) and just after sunset (sun elevation –10.6°). (B) A 62-second exposure taken on a moonless night in Death Valley National Park, California (Nikon D700, Nikon 20 mm f2.8 lens, f/2.8, ISO 6400). (C) A 148-second exposure taken three hours after sunset in the northwestern part of Yellowstone National Park (Nikon D70, Nikkor 20-mm lens, f/2.8, ISO 400). An almost full moon had recently risen on the eastern horizon. The scene appears as it would during the day (with the exception of the stars). Panel A adapted from Johnsen *et al*. (2006); panel C by Joseph Shaw, used with kind permission.

spectral absorption characteristics of chlorophyll and other pigments in the leaves. The 'greenish' light so produced is particularly noticeable on a sunny spring day in a deciduous forest. On overcast days, all these spectral variations tend to narrow, converging on an irradiance spectrum similar to that found in an extensive clearing. As pioneering visual ecologist John
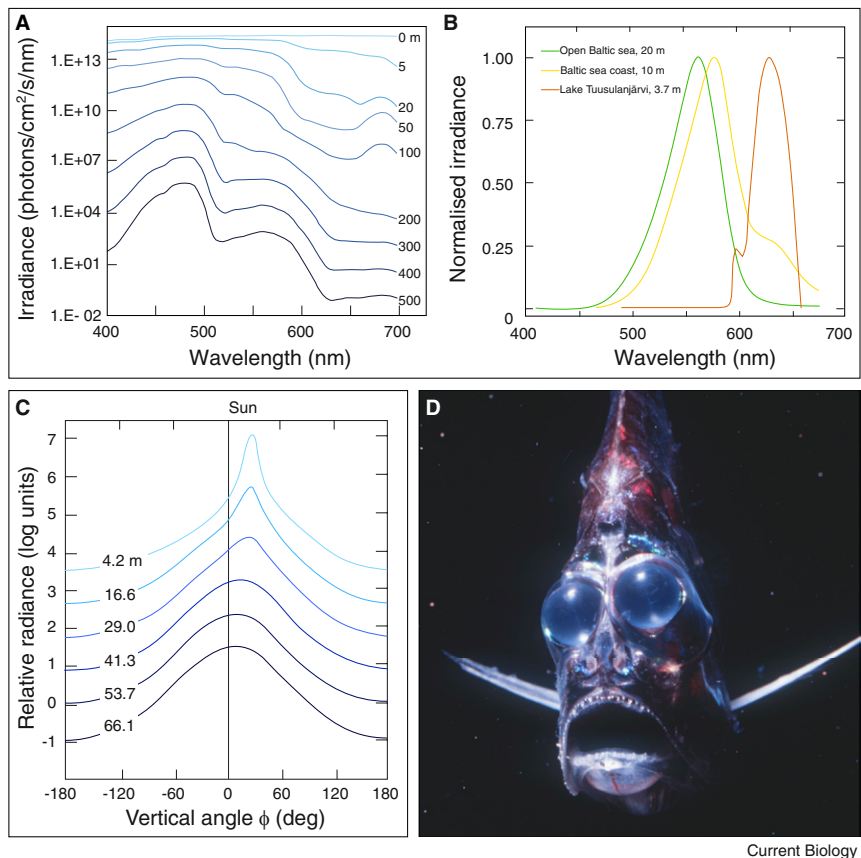
Figure 2. The spectral and spatial properties of light in aquatic habitats.
(A) Modelled downwelling irradiance spectrum as a function of depth (in metres) in the clear ocean of the equatorial Pacific that accounts for the absorption and scattering of light by water as well as for the fluorescence and concentration of chlorophyll and the presence of Raman scattering (where a small fraction of the 480 nm photons are converted to long-wavelength photons of lower energy). Adapted from Cronin *et al.* (2014). (B) Normalised irradiance spectra in three red-shifted aquatic habitats in Finland: in open (20 m depth) and coastal (10 m depth) areas of the Baltic Sea and in the inland lake Tuusulanjärvi (3.7 m depth). Data from Jokela-Määttä *et al.* (2007). (C) The change in the radiance distribution of green light with depth (shown in m) in Lake Pend Oreille. ϕ is the angle relative to vertical (0° = vertical, ±180° = horizontal). The distribution is skewed in the direction of the sun near the surface, but becomes more symmetric with increasing depth. In Lake Pend Oreille it becomes perfectly symmetric (asymptotic) at approximately 100 m. Diagrams adapted from Jerlov (1976) using classic data obtained by John E. Tyler in 1958. (D) A hatchet fish (of unknown species) with large dorsally-directed tubular eyes. Image ©Monterey Bay Aquarium, photo by David J. Wrobel, used with kind permission.

Endler first noted, the distinct variations found in forest light environments may have implications for visual camouflage and signalling — depending on its colouration, an animal that is camouflaged in one forest light environment may be less so in another. And visual signals may be more (or less) obvious for conspecifics (and predators) in one forest environment than in another. A forest animal may thus choose one light environment to maximise the efficacy of a visual signal aimed at a conspecific, while a short time later retreating to another in order to maximise its camouflage and thus reduce the risk of predation.

Aquatic light environments
Compared to aquatic habitats, however, variations in the intensity and spectrum of light in terrestrial habitats are quite modest. This is because water, in contrast to air, has a profound effect on the transmission of light. Water is a strong absorber of light, and associated particulate matter is a strong scatterer, both processes dramatically reducing the intensity, spectral composition, angular distribution and degree of polarisation of light with increasing depth. These significant variations in aquatic light with depth are reflected in equally significant variations in the eyes of aquatic animals.

Intensity
The absorption and scattering of light by water, phytoplankton and dissolved organic matter dramatically decreases the intensity of downwelling irradiance with depth. Even in a clear ocean, the irradiance intensity at 480 nm is reduced by about 2.5 log units within the first 100 m (Figure 2A). Below this depth irradiance declines less rapidly: about 1.5 orders of magnitude for every 100 m of depth (Figure 2A). It reaches starlight levels (during the day) by approximately 450–500 m. Below 1000 m (which defines the lower boundary of the mesopelagic zone) almost no daylight penetrates, certainly insufficient to be seen by the vast majority of deep-sea animals.

Eyes built to reliably see objects in the mesopelagic zone, illuminated by increasingly dim extended light, tend to become larger with depth and to develop wider pupils. They also tend to increasingly sacrifice spatial resolution by spatially summing signals from larger groups of neighbouring photoreceptors, thereby creating a brighter but coarser visual scene. Increases in eye size, however, are governed by a law of diminishing returns — the performance returns of having a larger eye are lower the larger the eye is to start with. This reduced performance return is exacerbated by the fact that eyes are also energetically expensive, larger eyes obviously more so. In fact it turns out that, for detecting objects illuminated by dim downwelling daylight (like prey and conspecifics), eyes larger than about 9 cm in diameter are seldom warranted.

Such eyes are found in large swordfishes, and eyes larger than this have only been found in one other group of aquatic animals — giant deep-sea squid. The massive 30 cm diameter eyes of deep-sea squid, like the colossal squid *Mesonychoteuthis hamiltoni* and the giant deep-sea squid *Architeuthis dux*, reach this size because they have not evolved to detect objects illuminated by the dim downwelling daylight. Instead, the benefit of such giant eyes seems to be the detection of the faint extended clouds of planktonic bioluminescence triggered by the swimming of their major predator, the sperm whale,

thus providing them with an 'early warning system' and the best chances of escape.

Colour

In a clear ocean, water is most transparent to blue light of wavelength around 480 nm (Figure 2A). Thus, clear oceanic light is predominantly blue in colour, although biologically relevant intensities of both shorter and longer wavelength light remain down to several hundred metres. As a result of the presence of sediments, phytoplankton and dissolved organic material, coastal waters and freshwater creeks and lakes may selectively absorb other wavelengths of light and appear more yellow-green, orange or brown in colour (Figure 2B).

Not surprisingly, the photoreceptors of animals living in these spectrally different light environments have visual pigments whose absorption spectra are reasonably well matched to the colour of the downwelling light. The obvious benefit of this match is an increased photon catch and higher sensitivity. For instance, the great majority (89%) of deep-sea fishes have an all-rod retina containing a single visual pigment with absorption peak wavelength (λ_{max}) in the range 468–494 nm, a range that is well matched to the near-monochromatic colour of downwelling oceanic light. The photoreceptors of cephalopods (λ_{max}: 470–480 nm), and to a lesser extent deep-sea crustaceans (λ_{max}: 480–540 nm), are similarly well matched.

Fishes living in yellow-green coastal waters and inland freshwater lakes tend instead to possess photoreceptors of longer λ_{max}. Indeed, one of the classes of cone photoreceptors in the pond-living goldfish *Carassius auratus* has a λ_{max} at 625 nm, one of the longest values known. Even within a single species (for example, the nine-spined stickleback *Pungitius pungitius*), individuals living in yellower waters may have visual pigments that are red-shifted relative to individuals living in bluer waters (shifts induced by changes in the relative proportions of the A1 and A2 chromophores). Paradoxically, however, these values of λ_{max} are often far shorter than the dominant wavelengths of aquatic light present in the habitat. One explanation for this is that the longer the λ_{max} of a visual pigment, the more susceptible the pigment is to thermal activation (in addition to light activation). This contaminating thermal noise could easily overwhelm the increased photon catch that the longer λ_{max} would otherwise bestow — the resulting λ_{max} is thus a compromise between maximising signal and minimising noise.

An impressive exception to the usual matching of vision to the prevailing light environment is found among three species of deep-sea dragonfishes (Family Stomiidae). These remarkable fishes have the unique ability to both produce and see far-red bioluminescent light (of wavelength beyond 700 nm), a light that is invisible to essentially all other deep-sea creatures, including the major predators of dragonfishes (although recent measurements amazingly suggest that one predator, the lanternfish *Bolinichthys longipes*, may actually be able to see it). Dragonfish eyes detect this unique red bioluminescence using a sensitising pigment that is most absorbent at 670 nm and that is based (quite remarkably) on chlorophyll-derived compounds originating in their copepod prey. Even though these long wavelengths are rapidly absorbed in water — limiting their useful range to less than 2 m — dragonfishes have the distinct advantage of possessing a 'private waveband' that may be used for secretly signalling to one another or for covertly illuminating their prey.

Polarisation

In still waters, the pattern of polarised light across the dome of the sky — a pattern used by many animals for navigation — is visible beneath the water surface, but turbidity and the presence of waves can degrade the pattern significantly. As a result of scattering from water molecules, there is also an underwater 'space light' visible both from below and from the side. This space light is strongly polarised in the horizontal plane, but the degree of polarisation declines rapidly with depth, falling to a constant value of between 13% and 38% below the so-called asymptotic depth (see below). Thus, polarised light is potentially available for vision throughout the mesopelagic zone, although it is probably most exploited in the epipelagic zone (the upper 200 m).

In clearer water, the space light's degree of polarisation is higher. Interestingly, fish that attempt to camouflage themselves by having mirror-like silvery flanks (see below) have little chance of remaining cryptic if the viewer has the ability to distinguish polarised light (such as a squid). This is because the mirrors change the polarisation of the reflected incident light; for a viewer without polarisation vision this change would not be visible, but for a squid the fish would be highly visible.

Angular distribution

With increasing depth in clear water, almost all of the daylight available for vision comes increasingly from above (Figure 2C). This radiance distribution is affected by the position of the sun in shallow water, but this influence declines with depth, disappearing altogether below the so-called 'asymptotic depth'. Below this depth —~200 m in the clearest water — the radiance distribution is vertically symmetric. In Lake Pend Oreille (Idaho, USA) it occurs at ~100 m. At this depth space light originating laterally ($\phi = \pm 90°$ in Fig. 2C) and from below ($\phi = \pm 180°$ in Figure 2C) is respectively about 40 times and 300 times dimmer than light originating directly above ($\phi = 0°$ in Figure 2C).

But regardless of the body of water in question, dim down-welling daylight provides a backdrop against which aquatic animals can spot animals floating above, or against which they themselves can be seen from below. In deep water, the most significant light sources in other directions would be bioluminescent. Not surprisingly, many aquatic animals that strain to maximise the contrast of objects seen in this dim dorsal extended light field have large eyes pointing directly upwards. Mesopelagic hatchet fishes provide a splendid example (Figure 2D): animals being viewed from below have evolved various mechanisms to remove their silhouettes and avoid detection, including transparency, silvered body flanks and the possession of ventral photophores that produce a fairly good mimic of the spectrum, intensity and angular

distribution of the surrounding downwelling light.

Deep-sea fishes that have instead evolved to detect bioluminescent point sources have eyes constructed accordingly, typically having a high spatial resolution provided by a retinal area of tightly packed visual cells arranged in a deep pit-like fovea. Their eyes, though, are often quite small, with pupils only as large as necessary to detect points of light at ecologically meaningful distances, which in the nutritionally impoverished deep may only be a few body lengths.

Further reading
Cronin, T.W., Johnsen, S., Marshall, N.J. and Warrant, E.J. (2014). Visual Ecology. (New Jersey: Princeton University Press). In press.
Douglas, R.H., Partridge, J.C., Dulai, K., Hunt, D., Mullineaux, C.W., Tauber, A.Y., and Hynninen, P.H. (1998). Dragon fish see using chlorophyll. Nature 393, 423–424.
Douglas, R.H., Hunt, D.M., and Bowmaker, J.K. (2003). Spectral sensitivity tuning in the deep-sea. In Sensory Processing in Aquatic Environments, S.P. Collin and N.J. Marshall, eds. (New York: Springer), pp. 323–342.
Endler, J.A. (1993). The color of light in forests and its implications. Ecol. Monog. 63, 2–27.
Jerlov, N.G. (1976). Marine Optics. (Amsterdam: Elsevier).
Johnsen, S. (2012). The Optics of Life. (New Jersey: Princeton University Press).
Johnsen, S., Kelber, A., Warrant, E.J., Sweeney, A.M., Widder, E.A., Lee, R.L. Jr., and Hernández-Andrés, J. (2006). Crepuscular and nocturnal illumination and its effects on color perception by the nocturnal hawkmoth *Deilephila elpenor*. J. Exp. Biol. 209, 789–800.
Jokela-Määttä, Smura, T., Aaltonen, A., Ala-Laurila, P., and Donner K. (2007). Visual pigments of Baltic Sea fishes of marine and limnic origin. Vis. Neurosci. 24, 389–398.
Lythgoe, J.N. (1979). The Ecology of Vision. (Oxford: Clarendon Press).
Nilsson, D.E., Warrant, E.J., Johnsen, S., Hanlon, R., and Shashar, N. (2012). A unique advantage for giant eyes in giant squid. Curr. Biol. 22, 683–688.
Saarinen, P., Pahlberg, J., Herczeg, G., Viljanen, M., Karjalainen, M., Shikano, T., Merilä, J. and Donner, K. (2012). Spectral tuning by selective chromophore uptake in rods and cones of eight populations of nine-spined stickleback (*Pungitius pungitius*). J. Exp. Biol. 215, 2760–2773.
Shashar, N., Hagan, R., Boal, J.G., and Hanlon, R.T. (2000). Cuttlefish use polarization sensitivity in predation on silvery fish. Vision Res. 40, 71–75.
Warrant, E.J. (2008). Nocturnal vision. In The Senses: A Comprehensive Reference (Vol. 2: Vision II), T. Albright and R.H. Masland, vol. eds.; A.I. Basbaum, A. Kaneko, G.M. Shepherd and G. Westheimer, ser. eds. (Oxford: Academic Press), pp. 53–86.
Warrant, E.J., and Locket, N. A. (2004). Vision in the deep sea. Biol. Rev. 79, 671–712.
Wehner, R., and Labhart, T. (2006). Polarisation vision. In Invertebrate Vision, E.J. Warrant and D.E. Nilsson, eds. (Cambridge: Cambridge University Press), pp. 167–210.

[1]Department of Biology, University of Lund, Sölvegatan 35, S-22362 Lund, Sweden.
[2]Department of Biology, Duke University, Durham, NC 27708, USA.
*E-mail: Eric.Warrant@biol.lu.se

Neanderthal and Denisovan retroviruses in modern humans

Emanuele Marchi[1,#], **Alex Kanapin**[2,#], **Matthew Byott**[3], **Gkikas Magiorkinis**[1,4,*] **and Robert Belshaw**[3,*]

In the June 5th 2012 issue of *Current Biology*, Agoni et al. [1] reported finding 14 endogenous retrovirus (ERV) loci in the genome sequences of Neanderthal and/or Denisovan fossils (both ~40,000 years old) that are not found in the human reference genome sequence. The authors [1] concluded that these retroviruses were infecting the germline of these archaic hominins at or subsequent to their divergence from modern humans (~400,000 years ago). However, in our search for unfixed ERVs in the modern human population, we have found most of these loci. We explain this apparent contradiction using population genetic theory and suggest that it illustrates an important phenomenon for the study of transposable elements such as ERVs.

The genomes of extinct human groups (archaic hominins), such as Neanderthals, are now available with high throughput sequencing technology, which can produce millions of short (~100 base) sequences called reads from fossil bone or teeth. An analysis of a Neanderthal and a Denisovan genome identified many reads that contained sequences of viral origin, similar to known integrations of retroviruses into the germline of modern humans [1]. Such so-called endogenous retroviruses (or ERVs) are common, making up ~5% of our genome. Some of the reads spanned the integration site of an ERV, called here a locus, and thus were part viral DNA and part archaic hominin DNA (Figure 1). In some cases, the authors [1] did not find an ERV at the corresponding coordinate in the human genome reference sequence. Instead they found the pre-integration site, which is the sequence that existed before the virus inserted a copy of itself into the chromosome. All of these loci belonged to one ERV lineage (family), called HERVK(HML2) or HERVK, which is the only lineage that has continued

to replicate within humans in the last few million years [2]. They concluded that these retroviruses had infected the germline of the archaic hominins either after their divergence from modern humans (~400,000 years ago) or immediately before divergence (with the integration and pre-integration sites then segregating differently in the lineages). However, while searching many new genome sequences of modern humans for ERVs, we have found most of these loci. For example, of the eight Denisovan loci for which Agoni et al. [1] were able to give precise genome coordinates, at least seven exist in modern humans. We have found six in an analysis of 67 cancer patient genomes (Figure 1), and examination of another study of 43 such genomes [3] shows all seven to be present (Supplemental information). One is K113 (19p12b), which is well-described and has a frequency of 16% in modern humans [2]. The four reported Denisovan loci lacking coordinates are within repetitive or unassembled regions of the genome, and we can neither confirm nor refute their presence in the modern human population: e.g. two loci are in transposable elements called Alu's, of which there are ~1,000,000 copies in the human genome (making up ~10% of the human genome sequence). When an ERV integrates into another transposable element, finding this ERV locus can be a formidable computational challenge because there are many paralogous copies of the integration site. Two additional loci were reported from the Neanderthal fossil, and we have found one of these.

It is unlikely that these ERV loci in the archaic hominins are contaminants from modern human DNA. Average coverage of the Denisovan genome was only about twofold and the contamination rate among the reads was estimated using several approaches to have been less than 1% [4]. We believe that the explanation lies in fundamental population genetics. With the exception of co-opted ERV loci such as syncytins [5], which could increase in frequency due to positive selection, we assume ERV loci become common by genetic drift, and the average time for a neutral allele to go to fixation is $4N_e$ generations (where N_e is the effective population size). Given estimates of long-term human generation time and population size [6], this is ~800,000 years. The population divergence of modern humans from the Denisovan/Neanderthal